Supporting information

Silver incorporated SeTe nanoparticles with enhanced photothermal and photodynamic properties for synergistic effects on anti-bacteria and wound healing

Irfan Ullah,[ad] Shahin Shah Khan,[ad] Waqar Ahmad,[a] Luo Liu,[a] Ahmed Rady,[b] Badr Aldahmash,[b] Changyuan Yu,*[a] and Yushu Wang*[c]

[a,] College of Life Science and Technology

Beijing University of Chemical Technology

Beijing 100029, China

Email: yucy@mail.buct.edu.cn

[b.]Department of Zoology, College of Science

King Saud University

P.O. Box 2455, Riyadh 11451, Saudi Arabia.

[c.]School of Pharmaceutical Sciences

Southern Medical University

No. 1023, South Shatai Road

Guangzhou 510515, China

Email: wysmjeda@gmail.com

[d.] I. Ulah and S. S. Khan contributed equally to this work.

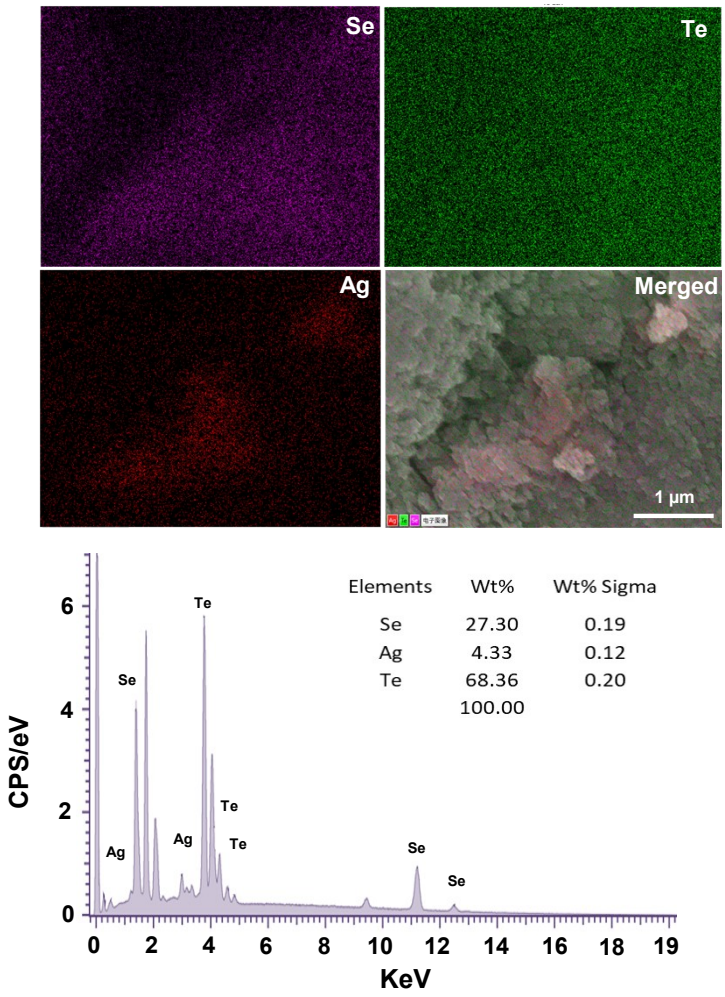

Fig. S1. Representative elements of Se, Te, and Ag mapping images and EDS spectra of SeTe-Ag NPs.

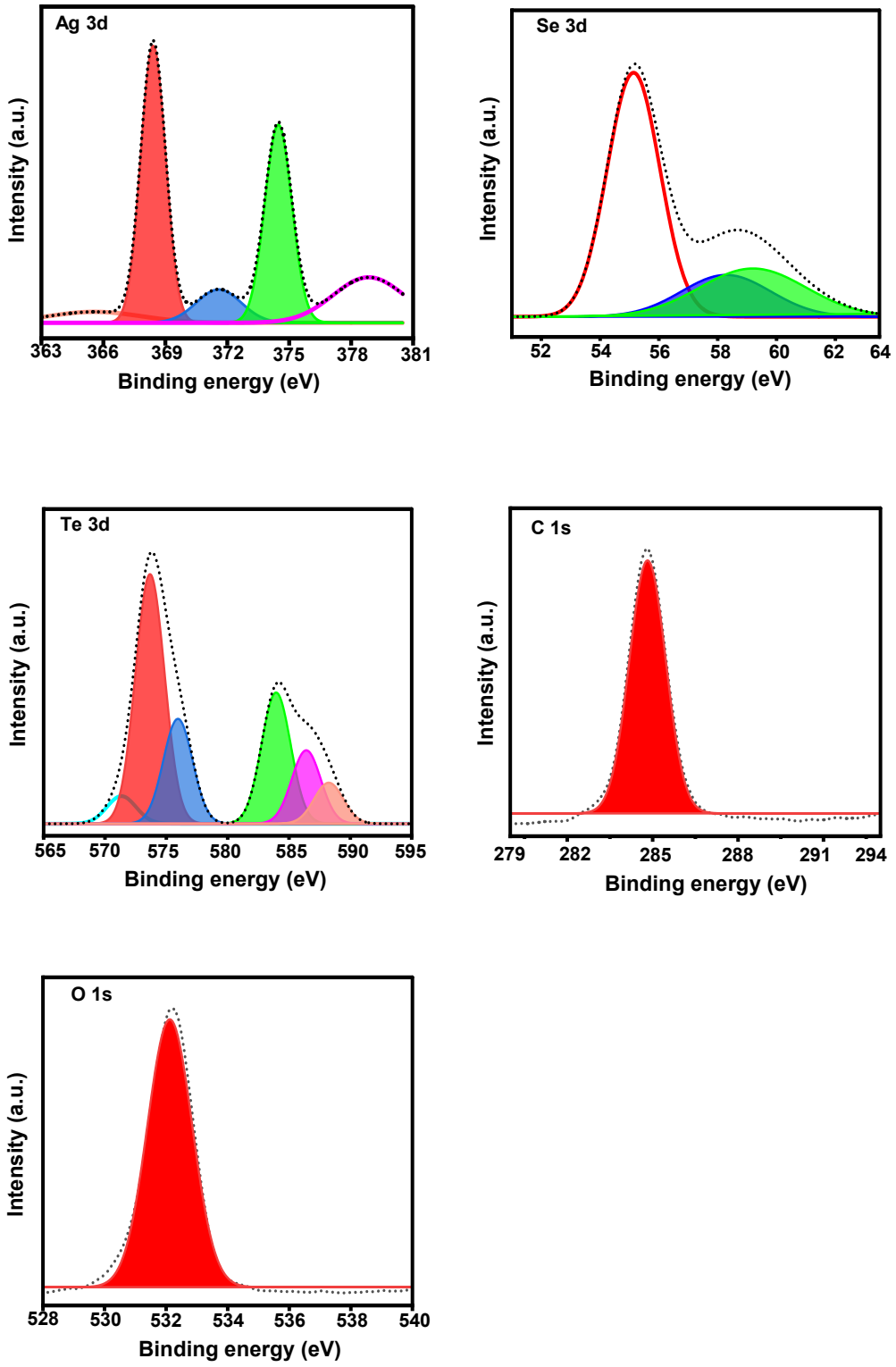

Fig. S2. XPS elemental spectra of Ag 3d, Se 3d, Te 3d, C1s and O1s of SeTe-Ag NPs.

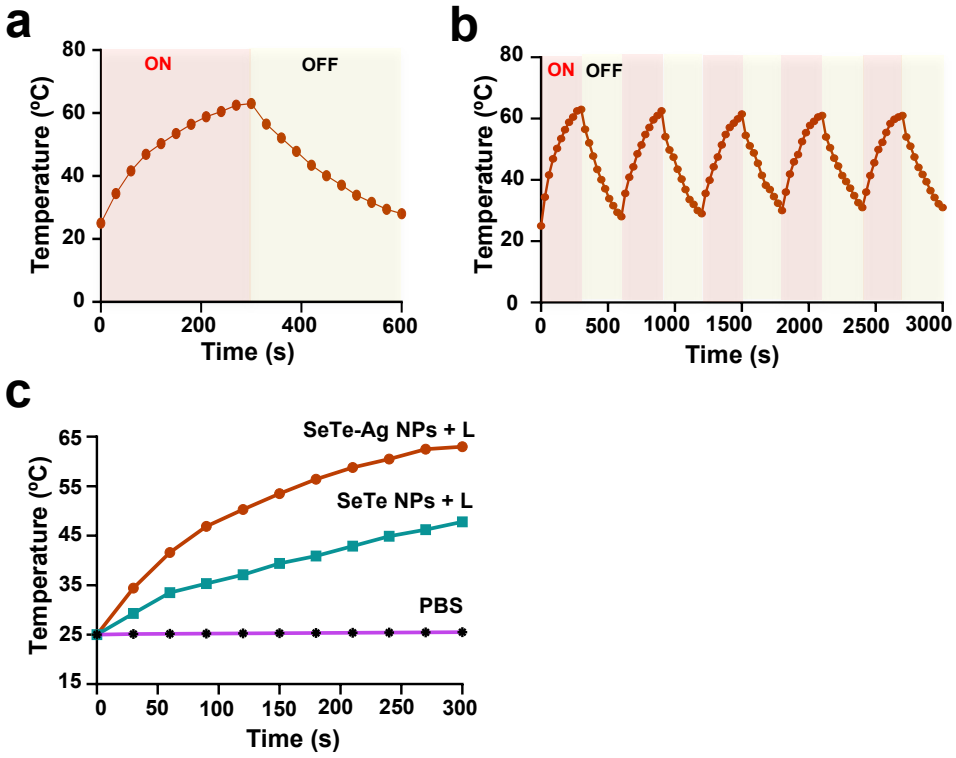

Fig. S3. Photothermal performance of SeTe-Ag NPs. (a, b) Single and five cycles of heating and cooling of SeTe-Ag NPs with NIR laser irradiation for five minutes ON and then OFF, and (b) comparative study of PBS, SeTe NPs and SeTe-Ag NPs after NIR laser irradiation.

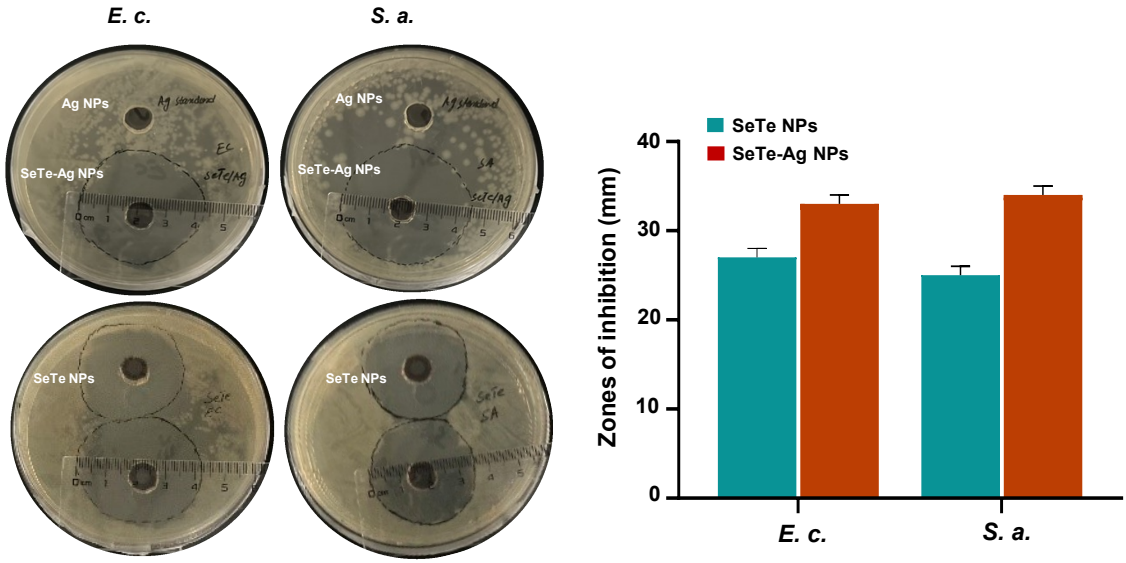

Fig. S4. Representative images and quantitative results for the zones of inhibitions of Ag NPs, SeTe NPs and SeTe-Ag NPs against *E. coli* and *S. aureus.*

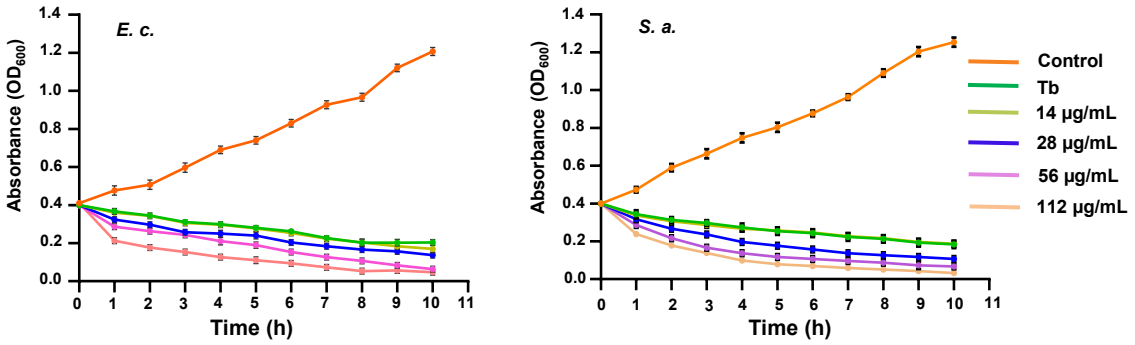

Fig. S5. Growth curves pattern of *E. coli* and *S. aureus* under the influence of tobramycin (Tb) in comparison with different concentrations of SeTe-Ag NPs.

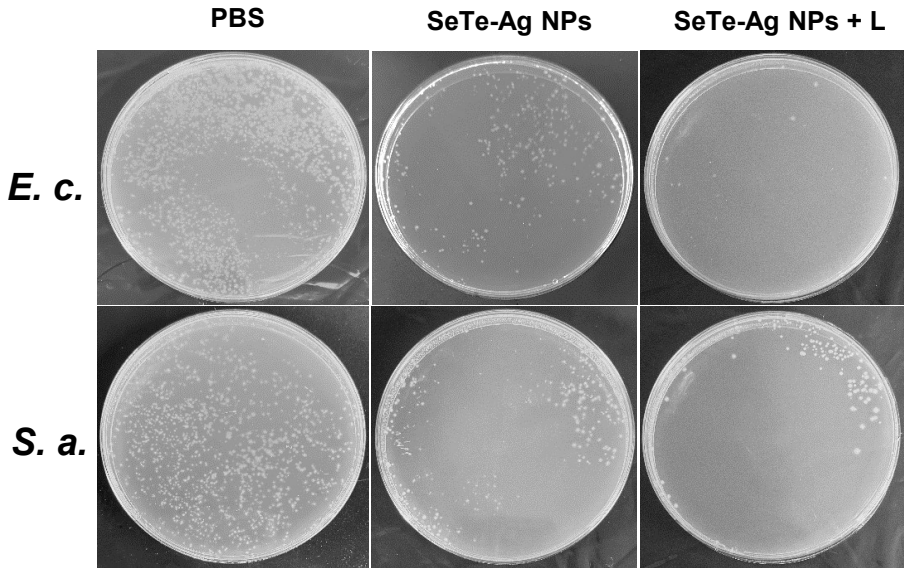

Fig. S6. Antibacterial activity of PBS, SeTe-Ag NPs, and SeTe-Ag NPs + L against *E. coli* and *S. aureus* using agar plate method.

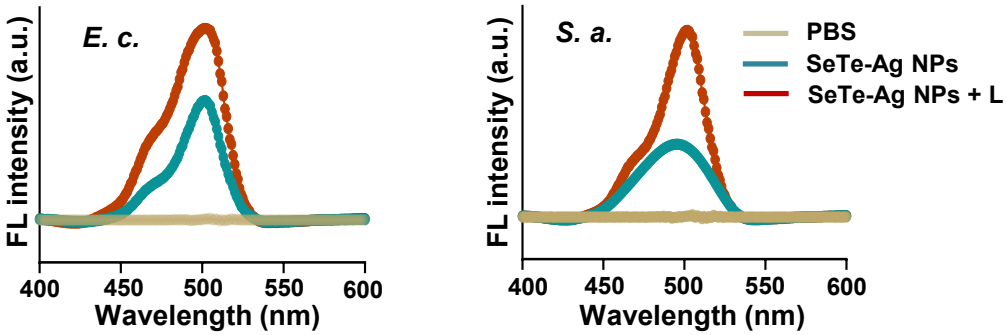

Fig. S7. Fluorescence (FL) intensity of bacterial intracellular ROS generation after treatment with PBS, SeTe-Ag NPs, and SeTe-Ag NPs + L.

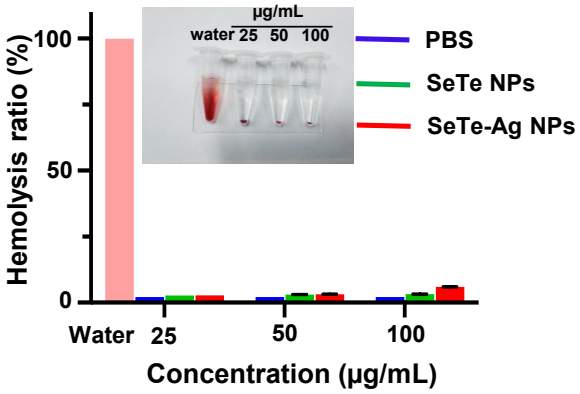

Fig. S8. Hemolysis ratio of SeTe NPs and SeTe-Ag NPs at different concentration.

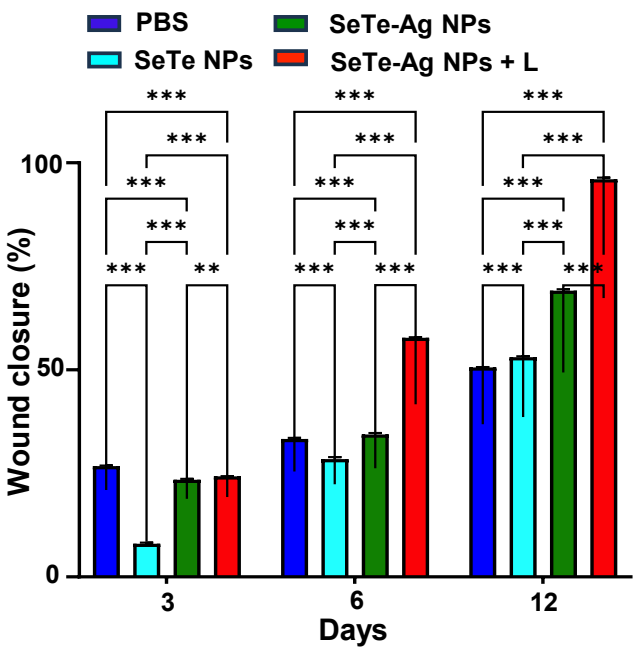

Fig. S9. Wound closure percentage of the healing wound after treatment with PBS, SeTe NPs, SeTe-Ag NPs and SeTe-Ag NPs + L.

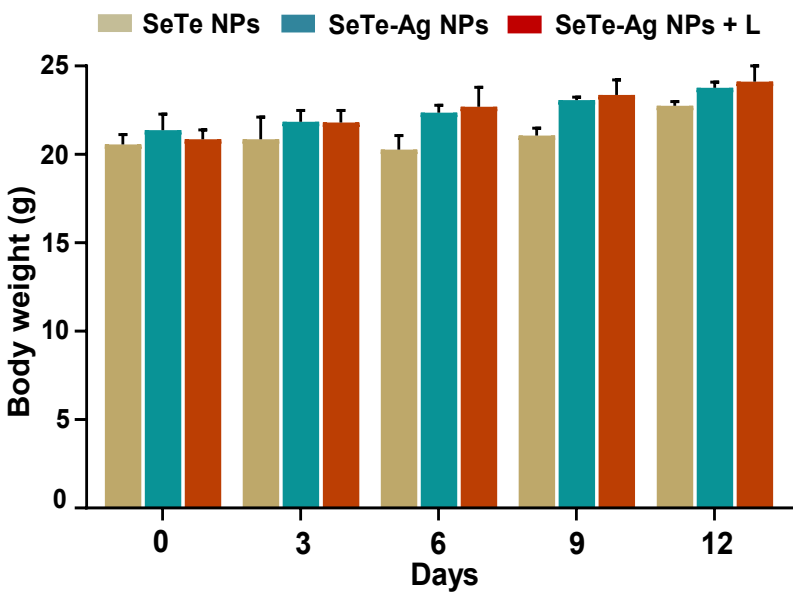

Fig. S10. Body weight of mice after treatment with SeTe NPs, SeTe-Ag NPs, and SeTe-Ag NPs + L on different days.

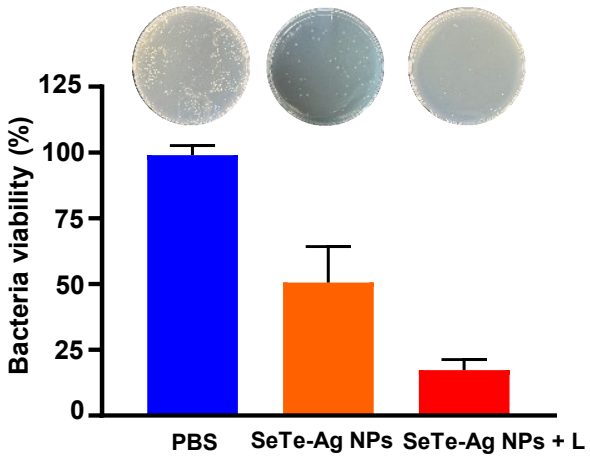

Fig. S11. Representative images and quantitative results of the bacteria from wound tissues of PBS, SeTe-Ag NPs, and SeTe-Ag NPs + L treatment groups.